

Robustness in Wireless Distributed Learning: An Information-Theoretic Analysis

Yangshuo He, Guanding Yu, and Huaiyu Dai

Abstract—In recent years, the application of artificial intelligence (AI) in wireless communications has demonstrated inherent robustness against wireless channel distortions. Most existing works empirically leverage this robustness to yield considerable performance gains through AI architectural designs. However, there is a lack of direct theoretical analysis of this robustness and its potential to enhance communication efficiency, which restricts the full exploitation of these advantages. In this paper, we adopt an information-theoretic approach to evaluate the robustness in wireless distributed learning by deriving an upper bound on the task performance loss due to imperfect wireless channels. Utilizing this insight, we define task outage probability and characterize the maximum transmission rate under task accuracy guarantees, referred to as the task-aware ϵ -capacity resulting from the robustness. To achieve the utility of the theoretical results in practical settings, we present an efficient algorithm for the approximation of the upper bound. Subsequently, we devise a robust training framework that optimizes the trade-off between robustness and task accuracy, enhancing the robustness against channel distortions. Extensive experiments validate the effectiveness of the proposed upper bound and task-aware ϵ -capacity and demonstrate that the proposed robust training framework achieves high robustness thus ensuring a high transmission rate while maintaining inference performance.

Index Terms—Information theory, wireless distributed learning, task-aware robustness

I. INTRODUCTION

As artificial intelligence (AI) applications are drawing intensive attention in the wireless communication system, wireless distributed learning emerges as a key characteristic of future communications. In wireless distributed learning, intelligent edge devices in wireless networks collaborate to achieve AI tasks by collecting, transmitting, and processing task-related data. The power of AI makes a paradigm shift from conventional bit-based metrics to task-aware metrics and requires novel approaches to enhance communication efficiency. In such a scenario, focusing on the AI task performance enables the transmitter and receiver to convey information that is both relevant to the task and robust to channel distortion. Hence, robust communication in terms of AI applications can be achieved even under lossy transmission. It has been shown that exploiting such robustness against wireless channel

noise provides a promising method to improve communication efficiency [1]. Moreover, the robustness in wireless distributed learning reveals the potential to transcend the limitation set by Shannon channel capacity. This fundamental evolution has stimulated various AI-based joint communication and learning designs that aim at robust and efficient communication in wireless distributed learning [2]–[4]. However, although many studies on architectural designs demonstrated the effectiveness of implicitly utilizing the inherent robustness of AI to enhance transmission rate, little attention has been paid to the theoretical analysis of such robustness, which hinders further development in this promising field. Therefore, it is essential to comprehend and quantify the inherent robustness in wireless distributed learning, thereby enabling the design of innovative and explainable methods to improve AI task performance.

A. Related Works

Various joint communication and learning designs emerge in light of the robustness in neural networks (NNs), such as the deep joint source-channel coding architecture for wireless image transmission in [3], where authors employed the NN-based encoder and decoder to jointly optimize the image reconstruction quality under wireless channel noise. Such a joint design was also applied in natural language processing for text transmission [2], which jointly trained the NN for both sentence similarity and transmission robustness. Beyond the goal of reconstruction in data-oriented communication, the authors in [1] introduced the joint communication and learning technique to task-aware communication that focuses on the accuracy of the AI tasks. However, it is worth noting that most of these works focus on the architecture design of NNs to achieve performance gain, primarily relying on empirical methods rather than theoretical foundations.

Some previous works attempted to theoretically analyze the performance gain of wireless distributed learning attributed to its robustness. By mimicking Shannon’s theory, the authors in [5] proposed a theoretical framework for semantic-level communication based on logical probability. Although the analysis is limited in the logical probability system, it sheds light on the theoretical research of integrating AI into wireless distributed learning. Adopting such an idea, the authors in [6] proposed the semantic channel capacity benefiting from NN’s robustness, which transcends the Shannon capacity. But there was no analytical solution and only numerical approximation by simulations was provided. To understand and exploit the intrinsic robustness within NNs, the authors in [1] utilized the information bottleneck (IB) framework to characterize the

This work was supported by the National Natural Science Foundation Program of China under Grant 62471434.

Yangshuo He and Guanding Yu are with the College of Information Science and Electronic Engineering, Zhejiang University, 38 Zheda Road, Hangzhou, China, 310027, email: {sugarhe@zju.edu.cn, yuguanding@zju.edu.cn} (*Corresponding author: Guanding Yu.*)

Huaiyu Dai is with the Department of Electrical and Computer Engineering, North Carolina State University, Raleigh, NC 27695 USA, e-mail: {hdai@ncsu.edu}.

trade-off between communication overhead and inference performance. The robustness is implicitly measured by the mutual information relevant to the task accuracy. A rate-distortion framework was proposed in [7] for the information source in AI applications. The framework characterizes the trade-off between the bit-level/task-level distortion and code rate. The task-oriented design based on IB reveals the potential of neural networks being robust to the imperfect wireless channel. Furthermore, the authors in [8] delved into the applications of the language model in wireless communication systems. A distortion-cost region was established as a critical metric for assessing task performance. In our previous work [9], we also investigate the inherent robustness in a multi-modal scenario. By employing the robustness verification problem, we evaluate the negative effect of wireless channels on task performance and thus measure the importance of each modality.

B. Motivations and Contributions

Integrating AI into wireless networks has shown great potential in mitigating channel distortions and enhancing transmission rates. Nevertheless, the absence of interpretable mathematical analysis on robustness may restrict the full utilization of these advancements to improve communication efficiency and task accuracy in wireless distributed learning. One attempt to evaluate the robustness in wireless distributed learning is to introduce information theory into AI tasks. For example, [1] utilized mutual information to measure the task-aware robustness and incorporated the IB framework to improve the robustness against channel distortion. However, the mutual information trade-off in [1] provides an implicit evaluation of the robustness, which limits the effectiveness of this approach in improving robustness and leveraging its potential advantages for more aggressive transmission. Motivated by these limitations, we employ the information theory to directly examine the robustness in wireless distributed learning. This paper aims to derive a theoretical measure of the inherent robustness of a learning system against wireless distortions and shed light on its potential benefit of enabling a transmission rate higher than channel capacity. To fully exploit the advantages of this robustness, we further propose a robust training framework for wireless distributed learning. Our goal is to enhance the intrinsic robustness and improve communication efficiency, thereby maximizing the benefits of AI in wireless distributed learning. The main contributions are summarized as follows:

- We evaluate the inherent robustness in wireless distributed learning by deriving an upper bound of the performance degradation due to the imperfect wireless channels. Specifically, we leverage the loss function as a metric for task performance, which is generally applicable to various AI tasks such as classification and regression. The AI's capability of mitigating the negative effect of wireless channels could be inferred from its impact on the loss function. By incorporating the Donsker-Varadhan representation of the Kullback-Leiber (KL) divergence, we further establish an upper bound on the performance degradation.

- To leverage the robustness in wireless distributed learning for enhancing transmission rates, we propose the task-aware ϵ -capacity, defined under the conditions ensuring successful inferences. In particular, we introduce a concept of task outage based on the derived upper bound to characterize instances of failure in wireless distributed inference. Building on this framework, we further define the task-aware ϵ -achievable rate which captures the achievability of a transmission rate in terms of task accuracy. By deriving an upper bound on this rate, termed the task-aware ϵ -capacity, we highlight the communication efficiency gains attributed to the inherent robustness in wireless distributed learning. This theoretical gain substantiates the potential of utilizing robustness to increase transmission rate in a task-aware manner.
- Given that the mutual information term in the derived upper bound is often intractable for most AI tasks with high dimensional features, we provide a numerical estimation for it in the context of NNs. Under common assumptions in NNs, we employ the bootstrapping technique to calculate the mutual information and develop an efficient algorithm for its estimation. This approach allows for the practical application of the previously proposed robustness analysis. Specifically, we apply this approach to a wireless distributed learning system, demonstrating that the performance loss due to the imperfect wireless channel is upper bounded by the derived theoretical bound and showing its usage for the task outage probability and task-aware ϵ -capacity in a realistic setting.
- We propose a robust training framework that leverages the derived upper bound on the task performance degradation to improve the inherent robustness in wireless distributed learning. To this end, we design an objective function that balances the trade-off between robustness and task accuracy. Our formulation aims to minimize the adverse impact of imperfect wireless channels meanwhile maximizing task accuracy. The proposed framework ensures the model achieves high task-aware robustness and is capable of transmitting data at a rate beyond the capacity limit while maintaining the inference performance.

The rest of this paper is organized as follows. Section II introduces the system model of wireless distributed learning and formulates the performance loss resulting from the imperfect wireless channel. Section III presents the theoretical analysis of the inherent robustness in wireless distributed learning, including the derived upper bound of the performance loss and the channel capacity benefiting from this robustness. Section IV provides a numerical example of the theoretical results within the context of NNs validating their effectiveness. Section V proposes the robust training framework based on the theoretical analysis. Numerical simulations are summarized in Section VI. Finally, Section VII concludes this paper.

II. SYSTEM MODEL

As shown in Figure 1, we consider a standard setting of distributed learning in the context of wireless communication systems with one base station (BS) and one user equipment

(UE). Let $\mathcal{Z} = \mathcal{X} \times \mathcal{Y}$ denote the sample space. A learning algorithm $p(w|z)$ maps the sample $Z = (X, Y)$ drawn from the space \mathcal{Z} to the hypothesis $W \in \mathcal{W}$. The learning model $f^{(W)} : \mathcal{X} \rightarrow \mathcal{Y}$ outputs the target variable given input data¹. Within the setting of wireless distributed learning, the model is further separated into an encoder $f_e^{(W)}$ and a decoder $f_d^{(W)}$, deployed at the UE and BS respectively. The data X is encoded by the encoder to signal M and transmitted to the decoder over a wireless channel with side information S . In this study, we consider the channel state as side information, such as the channel state information in a practical wireless communication system. Hence, $s \in \mathcal{S}$ can describe a particular wireless channel and it follows the probability distribution $\mu(s)$. The decoder at the BS leverages the received signal \hat{M} for decoding and outputs the target result \hat{Y} . These random variables constitute the following Markov chain:

$$Y \rightarrow X \rightarrow M \rightarrow \hat{M} \rightarrow \hat{Y}. \quad (1)$$

In a standard distributed learning model without wireless communication, the Markov chain can be simplified as $Y \rightarrow X \rightarrow M \rightarrow \hat{Y}$.

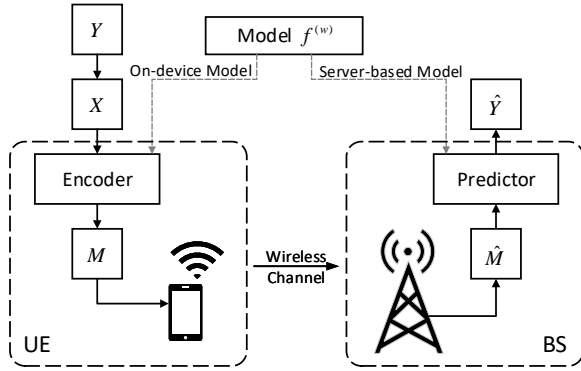


Fig. 1. System model.

The performance of the learning model $f^{(W)}$ can be generally measured by a loss function $l(f^{(w)}(x), y)$ that calculates the distance between the model output and the target variable. We formally define the loss function as $l : \mathcal{W} \times \mathcal{Z} \rightarrow \mathbb{R}^+$. First, we consider the performance of standard distributed learning. We denote the loss function for a model output as standard loss $\tilde{l} \triangleq l(\hat{y}, y)$. Given the joint distribution of $p(x, y)$, the *standard risk* is defined as

$$L \triangleq \mathbb{E}_{p(w|z)} \mathbb{E}_{p(x,y)} [l(W, Z)] = \mathbb{E}_{p(w,z)} [l(W, Z)]. \quad (2)$$

Note that in the above expression, the expectation is also taken over $p(w|z)$, as we are evaluating the risk on all learned posterior instead of a specific hypothesis w .

In the context of wireless communication systems, the noisy channel may affect the learning algorithm and the feature transmission, thus deteriorating the model performance. Upon a specific channel realization with side information s , we denote the loss function for a distorted output as wireless loss

$\hat{l} \triangleq l(\hat{y}, y)$. Given the joint distribution of the hypothesis and sample space conditioned on the side information, the *wireless risk* is defined as

$$L(s) \triangleq \mathbb{E}_{q(w,z|s)} [l(W, Z)]. \quad (3)$$

Therefore, the absolute difference between the wireless risk and the standard risk can be considered as the loss difference in the wireless environment. We denote the expectation on all channels as *wireless risk discrepancy*, which is given by

$$g(\mu, f) \triangleq \mathbb{E}_{\mu(s)} [|L(s) - L|], \quad (4)$$

where $\mu = \mu(s)$ is the probability distribution of the side information and $f = f^{(\cdot)}$ is the function of learning model.

The discrepancy can be viewed as a characterization of the model's robustness to the imperfect wireless channel and its meaning is twofold. First, via the power of deep learning, we can learn a model minimizing the difference to achieve better robustness against distortion in wireless communication systems. Second, a small discrepancy indicates that the model allows for more channel perturbation while maintaining task performance, thus a relatively high transmission rate can be adopted.

Traditional communication systems generally target error-free transmission or very small bit error rate (BER). However, error-free transmission doesn't necessarily align with the objectives of AI in a wireless scenario. The main goal of wireless distributed learning is to execute the task with sufficient precision, e.g., as measured by the accuracy in classification and the mean absolute error in regression. In the presence of wireless channel distortion, a task may still be completed successfully given the robustness of NNs. Therefore, we can transition from error-free to task-reliable transmission, exploiting the possible capacity gain in a wireless distributed learning system. To meet the task-reliable criterion, the system must ensure that the wireless risk discrepancy is negligible for the task's successful execution despite transmission errors.

III. THEORETICAL ANALYSIS OF THE ROBUSTNESS

In this section, we incorporate information theory to evaluate the robustness against channel distortions in wireless distributed learning. By investigating the discrepancy in loss functions, we derive an upper bound indicating the ability to mitigate the impact of channel noise. Subsequently, we investigate the benefit of such robustness in improving communication efficiency. In a task-aware manner, we introduce a novel concept of task outage and thus further propose a task-aware ϵ -capacity benefiting from the robustness in wireless distributed learning.

A. Upper Bound of Wireless Discrepancy

To carry out information-theoretic analysis, we revisit the wireless risk discrepancy $g(\mu, f)$ in (4), which measures the performance deterioration caused by the imperfect wireless channel. It can be viewed as the expected difference between distributions $q(w, z|s)$ and $p(w, z)$. Therefore, Kullback-Leibler (KL) divergence $D_{\text{KL}}(\cdot || \cdot)$ serves as a useful tool to measure the distance between q and p . We leverage the

¹In neural network settings, the function of learning model $f^{(W)}$ represents the network architecture while hypothesis W represents the weights.

Donsker-Varadhan variational representation of KL divergence in [10] as the following lemma.

Lemma 1. *For any two probability measures π and ρ defined on a common measurable space (Ω, \mathcal{F}) . Suppose that π is absolutely continuous with respect to ρ , i.e., for every event A , if $\pi(A) = 0$ then $\rho(A) = 0$. Then*

$$D_{\text{KL}}(\pi||\rho) = \sup_{F \in \mathcal{F}} \left\{ \int_{\Omega} F d\pi - \log \int_{\Omega} e^F d\rho \right\}, \quad (5)$$

where the supremum is taken over all measurable functions F , such that F is integrable under π and e^F is integrable under ρ .

We further assume that the loss function $l(w, z)$ is σ -sub-Gaussian² on distribution $p(w, z)$, which can be easily fulfilled by using a clipped loss function [11] [12]. Applying (5) with $\pi = q(w, z|s)$, $\rho = p(w, z)$, and $F = \lambda l(w, z)$, we have the following theorem.

Theorem 1. *If the loss function $l(w, z)$ is σ -sub-Gaussian on distribution $p(w, z)$, then the wireless risk discrepancy is upper bounded by*

$$g(\mu, f) \leq \sigma \sqrt{2I(W, Z; S)} \triangleq G. \quad (6)$$

Proof. From (5), we know that for any $\lambda \in \mathbb{R}$,

$$\begin{aligned} D_{\text{KL}}(q(w, z|s)||p(w, z)) &\geq \mathbb{E}_q[\lambda l(W, Z)] - \frac{\lambda^2 \sigma^2}{2} \\ &\geq \lambda (\mathbb{E}_q[l(W, Z)] - \mathbb{E}_p[l(W, Z)]) - \frac{\lambda^2 \sigma^2}{2}. \end{aligned} \quad (7)$$

For simple notation, we denote $D_{\text{KL}}(q(w, z|s)||p(w, z))$ as $D(q||p)$. Inequality (7) indicates a non-negative parabola in λ as follows

$$\frac{\sigma^2}{2} \lambda^2 - (\mathbb{E}_q[l(W, Z)] - \mathbb{E}_p[l(W, Z)]) \lambda + D(q||p) \geq 0. \quad (8)$$

To ensure the non-negativity of the parabolic function, a non-positive discriminant is required

$$\frac{1}{2\sigma^2} (\mathbb{E}_q[l(W, Z)] - \mathbb{E}_p[l(W, Z)])^2 - D(q||p) \leq 0. \quad (9)$$

Taking the expectation of the square root under the side information distribution μ gives

$$\begin{aligned} \mathbb{E}_{\mu} [|\mathbb{E}_q[l(W, Z)] - \mathbb{E}_p[l(W, Z)]|] &\leq \mathbb{E}_{\mu} \left[\sqrt{2\sigma^2 D(q||p)} \right] \\ &\leq \sqrt{2\sigma^2 \mathbb{E}_{\mu} [D(q||p)]}, \end{aligned} \quad (10)$$

where the second inequality follows from Jensen's inequality. Note that the mutual information is the expectation of the KL divergence $I(W, Z; S) = \mathbb{E}_{\mu(s)} [D(q||p)]$, we can derive $g(\mu, f) \leq \sigma \sqrt{2I(W, Z; S)}$. \square

Theorem 1 provides an upper bound on the expected discrepancy between the wireless risk and the standard risk. The wireless risk discrepancy in (4) evaluates the deterioration of task performance caused by the wireless channel distortion.

²A random variable X is σ -sub-Gaussian on p if for all $\lambda \in \mathbb{R}$, $\log \mathbb{E}_p [e^{\lambda X}] \leq \lambda^2 \sigma^2 / 2$.

A small discrepancy indicates the model is relatively robust to the channel noise. Since the wireless risk discrepancy in (4) is untrackable during the training and inference process of wireless distributed learning, it is natural to utilize the derived upper bound $G = \sigma \sqrt{2I(W, Z; S)}$ as an alternative of the measurement of task-aware robustness. Minimizing the upper bound enables the model to transmit at a high rate beyond capacity while preserving task accuracy. Therefore, it is essential for the wireless distributed learning model to learn an optimal hypothesis that achieves a tight upper bound. In the following section, we will derive an efficient algorithm to estimate the upper bound in the NN scenario and propose a novel framework for robust inference in wireless distributed learning.

Remark 1. In the context of wireless distributed learning, it is worth noting that the loss difference vanishes upon achieving error-free transmission, i.e., transmission rate $R < C$. Additionally, if the mutual information $I(W, Z; S) = 0$, the wireless risk discrepancy also becomes zero. It suggests that (W, Z) is independent of side information S . In this scenario, the model is generalized to any wireless channel as analyzed in [13], thus accomplishing perfect inference in wireless distributed learning. However, the absolute independence is virtually unattainable. In practice, the learning algorithm can only find a model where the mutual information approaches zero.

Remark 2. Using the chain rule of mutual information, $I(W, Z; S)$ can be written as

$$I(W, Z; S) = I(Z; S) + I(W; S|Z), \quad (11)$$

and

$$I(W, Z; S) = I(W; S) + I(Z; S|W). \quad (12)$$

From (11), it can be observed that the sample Z consisting of input data X and target Y is independent of the wireless channel. Hence the first term $I(Z; S) = 0$ and the mutual information can be reduced to $I(W, Z; S) = I(W; S|Z)$. The first term in (12) represents the information of the channel contained in the learned hypothesis. From the perspective of probably approximately correct (PAC) [13], a small $I(W; S)$ mitigates over-fitting on a specific channel and thus increases robustness against wireless channels. The second term can be further written as $I(Z; S|W) = I(Y; S|W, X) + I(X; S|W)$, where $I(Y; S|W, X) = \mathbb{E}_{p(x, w, s)} [D_{\text{KL}}(p(y|x, w, s)||p(y|w, x))]$. In the classification problem, the cross-entropy between the wireless prediction $p(y|x, w, s)$ and the standard prediction $p(y|x, w)$ becomes $CE(p(y|x, w, s), p(y|x, w)) = H(p(y|x, w, s)) + D_{\text{KL}}(p(y|x, w, s)||p(y|w, x))$. Therefore, minimizing the mutual information $I(W, Z; S)$ is equivalent to reducing the distance between \hat{y} and \tilde{y} , thus mitigating the negative effect of the wireless channel.

Remark 3. In this part, we examine the achievability of the upper bound presented in Theorem 1. The sub-Gaussian condition takes an equal sign when the variable X is a Gaussian distribution with zero mean. The equality in the second inequality in (7) is achieved when the standard risk is zero,

i.e., $\mathbb{E}_p[l(W, Z)] = 0$. This condition implies that the model becomes perfect in standard distributed learning. However, this represents an idealized scenario that is generally unattainable in practical applications. It is further discerned from (9) that when the discriminant is zero, there is only one solution for the parabola, given by $\lambda_0 = \sqrt{2D_{\text{KL}}(q\|p)}/\sigma^2$. Finally, the Jensen's inequality in (10) becomes trivial when $D(q\|p)$ is constant. In this scenario, the two distributions $q(w, z|s)$ and $p(w, z)$ either are identical or have a fixed relationship, indicating perfect inference as analyzed in Remark 1. Therefore, the upper bound of the wireless performance gap in Theorem 1 is achieved when the model becomes perfect in both standard and wireless distributed learning and the loss function adheres to Gaussian distribution $l(w, z) \sim \mathcal{N}(0, \frac{\sigma^4}{2D_{\text{KL}}(q\|p)})$.

Remark 4. The existing information-theoretic analysis based on IB [1] utilizes $I(X; T)$ to measure the robustness of NNs in edge inference indirectly. Unlike such an analysis on the data flow $X \rightarrow T$ [14], the derived upper bound $I(W, Z; S)$ quantifies the information of the wireless channel contained in the network and directly reveals the robustness against wireless distortion. Moreover, our measure is invariant to the choice of activation functions, since it is not directly influenced by hidden representations like $I(X; T)$.

Remark 5. In our previous analysis, we assumed that the loss function $l(w, z)$ is σ -sub-Gaussian, enabling us to leverage the properties of sub-Gaussian distributions in deriving the upper bound. However, this assumption may be too strict in certain scenarios where the loss function exhibits heavier tails. To address this limitation, we extend our theoretical results to sub-Gamma distributions, which encompasses a broader class of loss functions.

A random variable X is said to be sub-Gamma if for all $0 < \lambda < c^{-1}$:

$$\log \mathbb{E} [e^{\lambda X}] \leq \frac{\lambda^2 \sigma^2}{2(1 - c\lambda)}, \quad (13)$$

where $\sigma > 0$ and $c > 0$ are parameters characterizing the variance and tail behavior, respectively. Sub-Gamma distributions generalize sub-Gaussian distributions (where $c = 0$) by allowing for heavier tails. Under this assumption, we can also derive an analogous upper bound on the performance degradation caused by imperfect wireless channels.

Corollary 1. *If the loss function $l(w, z)$ is (σ, c) -sub-Gamma on distribution $p(w, z)$, then the wireless risk discrepancy is upper bounded by*

$$\begin{aligned} \tilde{g}(\mu, f) &\triangleq \mathbb{E}_{\mu(s)} [L(S) - L] \\ &\leq \sigma \sqrt{2I(W, Z; S)} + cI(W, Z; S). \end{aligned} \quad (14)$$

The proof is provided in Appendix A. The upper bound in the sub-Gamma scenario differs slightly from (6). Specifically, we can only provide an upper bound on the discrepancy between wireless risk and stand risk rather than the absolute value in (4). To accommodate the more general loss functions, the resulting bound is relatively looser compared to the sub-Gaussian assumption. Such an extension broadens the applicability of our theoretical analysis of the inherent robustness in wireless distributed learning.

B. Task-aware ϵ -Capacity

The wireless risk discrepancy is a statistical measure averaged over the probability space and provides a general view. However, to delve deeper into the possible task-aware ϵ -capacity benefiting from the robustness, we pay special attention to each detailed event. Specifically, for an individual inference (z, w, s) , where z , w , and s represent a particular sample, hypothesis, and channel, respectively, the difference between the actual wireless loss $\hat{l}(\hat{y}(x, w, s), y)$ and the true risk L would possibly exceed the upper bound G in Theorem 1. This deviation depends on the variability of the performance deterioration across different realizations, and deviations could occur due to variable samples, hypotheses, and channel conditions.

To better analyze the probabilistic nature of wireless distributed learning, we introduce the concept of *task outage* as in [15] and [16], which extends the outage in conventional communication systems towards the domain of wireless distributed learning. The concept of outage is the event that occurs whenever the capacity falls below a target rate R [17]. However, given the robustness of NNs, lossy transmission is acceptable in wireless distributed learning as long as the performance is not severely affected. Therefore, we focus on the event that the instantaneous loss difference transcends the upper bound G of the wireless risk discrepancy.

Definition 1. For an individual wireless distributed learning (z, w, s) with a transmission rate R , a *task outage* occurs when the following condition is satisfied. Then we define a random variable E as the corresponding indicator

$$E = \mathbf{1} \left(\left| \hat{l}(\hat{y}_R(x, w, s), y) - L \right| \geq \sigma \sqrt{2I(W, Z; S)} \right), \quad (15)$$

where $\mathbf{1}(\cdot)$ is the indicator function, $\hat{y}_R(x, w, s) = f_d^{(w)}(\hat{m})$ is the output of the decoder, \hat{m} is the received signal that is transmitted through wireless channel s at rate R . The set of wireless loss that causes task outage can be written as $\mathcal{E} = \{\hat{l} : E = 1\}$. Thus, the task outage probability is expressed as

$$p_e \triangleq \Pr\{E = 1\}. \quad (16)$$

In the conventional communication system, [18] defines ϵ -achievable rate in the context of lossy transmission with error ϵ . Given the task outage probability, we adopt this notion and apply it to the lossy transmission in wireless distributed learning.

Definition 2. An (n, M, ϵ) code has block length n , M codewords, and task outage probability not larger than ϵ . $R \geq 0$ is a *task-aware ϵ -achievable rate* if, for every $\delta > 0$, there exist, for all sufficiently large n , (n, M, ϵ) codes with rate

$$\frac{\log M}{n} > R - \delta. \quad (17)$$

Theorem 2. *If $R \geq 0$ is task-aware ϵ -achievable, then*

$$R \leq \frac{1}{1 - \epsilon} C \triangleq C_\epsilon, \quad (18)$$

where $C = \liminf_{n \rightarrow \infty} \sup_{M^n} \frac{1}{n} I(M^n; \hat{M}^n)$ represents the Shannon's channel capacity. The maximum task-aware ϵ -achievable rate is called the *task-aware ϵ -capacity C_ϵ* .

Proof. A message J , drawn from the index set $\{1, 2, \dots, M\}$, is the output of the model encoder and results in the signal $M^n(J)$ by channel encoder. The received signal \hat{M}^n is used to guess the message by a channel decoder $\hat{J} = g(\hat{M}^n)$.

$$H(J|\hat{J}) \leq H(J, E|\hat{J}) \quad (19a)$$

$$= H(E|\hat{J}) + H(J|\hat{J}, E) \quad (19b)$$

$$\leq H(E) + H(J|\hat{J}, E) \quad (19c)$$

$$= H(E) + p_e H(J|\hat{J}, E = 1) \quad (19d)$$

$$+ (1 - p_e) H(J|\hat{J}, E = 0)$$

$$\leq H(E) + p_e H(J|\hat{J}, E = 1) \quad (19e)$$

$$\leq H(E) + p_e \log(|\mathcal{J}| - 1) \quad (19f)$$

$$\leq H(E) + \epsilon \log M, \quad (19g)$$

where (19a) is from data processing inequality, (19c) is due to the fact that conditioning can only decrease entropy, (19f) is because $H(J|\hat{J}, E = 1)$ is maximized when $p(J|\hat{J}, E = 1)$ is uniformly distributed, which yields to $\log(|\mathcal{J}| - 1)$. Hence, for any coding scheme,

$$\log M = H(J) \quad (20a)$$

$$= H(J|\hat{J}) + I(J; \hat{J}) \quad (20b)$$

$$\leq H(J|\hat{J}) + I(M^n; \hat{M}^n) \quad (20c)$$

$$\leq H(E) + \epsilon \log M + I(M^n; \hat{M}^n) \quad (20d)$$

$$\leq H(E) + \epsilon \log M + \sup_{M^n} I(M^n; \hat{M}^n), \quad (20e)$$

where (20a) is because J is uniformly distributed, (20c) is from data processing inequality, and (20d) is from the result obtained with (19). Therefore, for every $\delta > 0$

$$R - \delta < \frac{1}{1 - \epsilon} \left[\frac{1}{n} \sup_{M^n} I(M^n; \hat{M}^n) + \frac{H(E)}{n} \right], \quad (21)$$

which, in turn, implies

$$R \leq \frac{1}{1 - \epsilon} \liminf_{n \rightarrow \infty} \frac{1}{n} \sup_{M^n} I(M^n; \hat{M}^n). \quad (22)$$

□

Remark 6. It can be seen that the capacity gain falls back to Shannon's channel capacity when $\epsilon = 0$. In this scenario, the task outage would never occur, indicating that the wireless loss \hat{l} must fall within a bounded region $[L - G, L + G]$. Since loss functions are usually unbounded or semi-bounded distributions, $p_e = 0$ leads to $\hat{l} = \mathbb{E}[\hat{l}]$. Thus, it corresponds to the error-free transmission in Remark 1. On the contrary, the special case of $p_e = 1$ is unattainable for common distributions in AI applications, thus the capacity gain could not be infinite.

Remark 7. We can observe from (18) that the capacity gain increases with p_e . By exploring the definition of task outage probability $p_e = \Pr \left\{ \left| \hat{l} - L \right| \geq G \right\}$, we perceive p_e as a two-tailed probability of the distribution of \hat{l} . Several major factors contribute to the augmentation of probability.

- First, an increase in the variance of \hat{l} or the transition to a heavy-tailed distribution may be noted. This indicates a high BER in communication, which arises from a high

transmission rate. Therefore, with the increase of task achievable rate, a higher capacity gain could be obtained.

- Second, a small cut-off value G also contributes to the increase of two-tailed probability. As analyzed in Remark 2, a small wireless risk discrepancy upper bound G helps alleviate the over-fitting on a specific channel and thus enhances the model's robustness against the impact of wireless channels. Therefore, a high task-aware ϵ -capacity might be achieved despite the channel distortion.
- Third, the standard risk L moving closer towards the tails of the distribution may increase p_e . As a result, the wireless risk discrepancy approaches the upper bound G which implies the model's capability of fully exploiting the intrinsic robustness in wireless distributed learning. Thus, a more substantial capacity gain could be possible.

IV. NUMERICAL ESTIMATION OF UPPER BOUND

By deriving an information-theoretic upper bound for the performance deterioration, we shed light on how to exploit the task-aware ϵ -capacity from the robustness in wireless distributed learning. The key challenge is the calculation of $I(W; Z; S)$ in a practical setting. In this section, we address this issue by utilizing an NN-based model $f^{(W)}$ in wireless distributed learning as an example.

In the context of NNs, the hypothesis W represents the weights of the NN and the sample space \mathcal{Z} represents the dataset. As specified in Remark 2, we turn to estimate the conditional mutual information $I(W; S|Z)$ for convenience. It can be written as the expectation of the KL divergence between $p(w|s, z)$ and $p(w|z)$ as,

$$I(W; S|Z) = E_{p(s, z)} [D_{\text{KL}}(p(w|s, z) \| p(w|z))]. \quad (23)$$

Considering the Bayesian equation $p(w|s, z) = \frac{p(w|z)p(s|w, z)}{p(s|z)}$, $p(w|z)$ can be interpreted as prior knowledge of the weights depending on a given dataset z . Meanwhile, $p(w|s, z)$ represents the posterior distribution of the weights given a dataset z and the evidence of side information s . Prior $p(w|z)$ is the probability of NN's weights before learning about the wireless channel. Following the common assumption in deep learning theory, we assume both $p(w|z) = \mathcal{N}(w|\theta_z, \Sigma_z)$ and $p(w|s, z) = \mathcal{N}(w|\theta_{s, z}, \Sigma_{s, z})$ are Gaussian. The means $\theta_z, \theta_{s, z}$ are the yielded hypotheses of the learning algorithm given the corresponding knowledge. Thus, the KL divergence term has a closed-form expression as

$$D_{\text{KL}}(p(w|s, z) \| p(w|z)) = \frac{1}{2} \left[\log \frac{\det \Sigma_{s, z}}{\det \Sigma_z} - D + (\theta_{s, z} - \theta_z)^\top \Sigma_z^{-1} (\theta_{s, z} - \theta_z) + \text{tr} (\Sigma_z^{-1} \Sigma_{s, z}) \right], \quad (24)$$

where \det and tr represent the determinant and trace of a matrix, respectively, while D represents the dimension of weight w , which is a constant for a specific model $f^{(W)}$. For simplicity, we further assume the covariances of both the prior and the posterior are proportional, which is a common practice in PAC-Bayes analysis [19]. As a result, the logarithmic and trace terms in (24) become constant and the conditional mutual information can be expressed as

$$I(W; S|Z) \propto E_{p(s, z)} \left[(\theta_{s, z} - \theta_z)^\top \Sigma_z^{-1} (\theta_{s, z} - \theta_z) \right]. \quad (25)$$

Thus, the prior covariance can be approximated using bootstrapping [13] by

$$\Sigma_z \approx \frac{1}{K} \sum_{k=1}^K (\theta_{(s,z)_k} - \theta_{s,z}) (\theta_{(s,z)_k} - \theta_{s,z})^\top, \quad (26)$$

where $(s, z)_k$ is a bootstrap sampling set from space $\mathcal{S} \times \mathcal{Z}$ in the k -th experiment. During the training process of deep learning, it is prohibitive to learn weight $\theta_{(s,z)_k}$ from K bootstrapping samples. Therefore, we further utilize the influence function (IF) from robust statistic [20] to approximate the difference $\theta_{(s,z)_k} - \theta_{s,z}$.

Lemma 2 (Influence Function [21]). *Assume in Poisson bootstrapping that the sampling weights denoted by $\xi = (\xi_1, \dots, \xi_n)^\top$ follows a binomial distribution $\xi_i \sim \text{Binomial}(n, \frac{1}{n})$, where $\lim_{n \rightarrow \infty} \text{Binomial}(n, \frac{1}{n}) \rightarrow \text{Poisson}(1)$. Given new hypotheses $\hat{\theta}_{(s,z),\xi} \triangleq \arg \min_{\theta} \frac{1}{n} \sum_{i=1}^n \xi_i \hat{l}_i(\theta)$ ³ and $\hat{\theta}_{s,z} \triangleq \arg \min_{\theta} \frac{1}{n} \sum_{i=1}^n \hat{l}_i(\theta)$, the approximation of difference is defined by*

$$\hat{\theta}_{(s,z),\xi} - \hat{\theta}_{s,z} \approx \frac{1}{n} \sum_{i=1}^n (\xi_i - 1) \psi_i = \frac{1}{n} \boldsymbol{\psi}^\top (\boldsymbol{\xi} - \mathbf{1}), \quad (27)$$

where $\psi_i = -\mathbf{H}_{\hat{\theta}_{s,z}}^{-1} \nabla_{\theta} \hat{l}_i(\hat{\theta}_{s,z})$ represents the IF, $\boldsymbol{\psi} = (\psi_1, \dots, \psi_n)^\top$ represents the collection of IFs, and $\mathbf{H}_{\hat{\theta}_{s,z}} = \frac{1}{n} \sum_{i=1}^n \nabla_{\theta}^2 \hat{l}_i(\hat{\theta}_{s,z})$ represents the Hessian matrix. As a result, the covariance can be approximated as

$$\begin{aligned} \Sigma_z &\approx \frac{1}{K} \sum_{k=1}^K \left(\hat{\theta}_{(s,z),\xi_k} - \hat{\theta}_{s,z} \right) \left(\hat{\theta}_{(s,z),\xi_k} - \hat{\theta}_{s,z} \right)^\top \\ &\approx \frac{1}{n} \mathbf{F}_{\hat{\theta}_{s,z}}^{-1}, \end{aligned} \quad (28)$$

where ξ_k represents the sampling weights in the k -th experiment and $\mathbf{F}_{\hat{\theta}_{s,z}}$ is the Fisher information matrix.

Now we are able to approximate the conditional mutual information in (25) as

$$\begin{aligned} I(W; S|Z) &\propto n \mathbb{E}_{p(s,z)} \left[(\theta_{s,z} - \theta_z)^\top \mathbf{F}_{\hat{\theta}_{s,z}}^{-1} (\theta_{s,z} - \theta_z) \right] \\ &\approx n (\bar{\theta}_{s,z} - \theta_z)^\top \mathbf{F}_{\hat{\theta}_{s,z}}^{-1} (\bar{\theta}_{s,z} - \theta_z), \end{aligned} \quad (29)$$

where we employ quadratic mean $\bar{\theta}_{s,z} = \sqrt{\frac{1}{K} \sum_{k=1}^K \hat{\theta}_{(s,z),\xi_k}^2}$ to better estimate $\theta_{s,z}$ in the expectation. In practice, we could pre-train a model in standard distributed learning to obtain θ_z , and we denote $\Delta\theta = \bar{\theta}_{s,z} - \theta_z$. By expanding the Fisher information matrix, (29) can be simplified as

$$\begin{aligned} I(W; S|Z) &\propto n \Delta\theta^\top \left[\frac{1}{T} \sum_{t=1}^T \nabla_{\theta} \hat{l}_t(\hat{\theta}_{s,z}) \nabla_{\theta} \hat{l}_t(\hat{\theta}_{s,z})^\top \right]^{-1} \Delta\theta \\ &= \frac{n}{T} \sum_{t=1}^T \left[\Delta\theta^\top \nabla_{\theta} \hat{l}_t(\hat{\theta}_{s,z}) \right]^2 \triangleq \tilde{I}(W; S|Z), \end{aligned} \quad (30)$$

³To simplify the notation, we denote the loss function for wireless distorted output with weight θ as $\hat{l}_i(\theta) = l(\hat{y}, y)$, where \hat{y} is the distorted output of model $f^{(\theta)}$.

where n denotes the number of samples and T denotes the number of iterations to estimate Fisher information. In this way, the complexity of estimating the conditional mutual information becomes $O(DT)$, and the corresponding algorithm is summarized in Algorithm 1.

Algorithm 1 Efficient approximation of conditional mutual information $I(W; S|Z)$

Require: Number of samples n , number of batches B , number of estimation iterations T , average parameters (ρ, K) .

Ensure: Approximated $\tilde{I}(W; S|Z)$.

- 1: Pre-train in standard distributed learning, $\theta_z \leftarrow p(w|z)$.
 - 2: **for** $t = 1 : B$ **do**
 - 3: Train in wireless distributed learning, calculate and store the gradient ∇l_t .
 - 4: Back-propagation and update weight $\hat{\theta}_t$.
 - 5: Apply moving average hypotheses over K iterations $\bar{\theta}_t \leftarrow \sqrt{\rho \bar{\theta}_{t-1}^2 + \frac{1-\rho}{K} \sum_{k=0}^{K-1} \hat{\theta}_{t-k}^2}$.
 - 6: **end for**
 - 7: $\Delta\theta \leftarrow \bar{\theta}_B - \theta_z$, $\Delta F \leftarrow 0$.
 - 8: **for** $t = 1 : T$ **do**
 - 9: $\Delta F_t \leftarrow \Delta F_{t-1} + (\Delta\theta^\top \nabla l_t)^2$.
 - 10: **end for**
 - 11: $\tilde{I}(W; S|Z) \leftarrow \frac{n}{T} \Delta F_T$.
-

To validate the effectiveness of the proposed task-aware ϵ -capacity in Section III, we utilize a classic binary classification dataset of ASIRRA Cats & Dogs [22] and employ a 6-layer convolutional neural network (CNN) for the distributed wireless learning system. Specifically, the encoder $f_e^{(w)}$ at the UE is comprised of the first 3 layers and the decoder $f_d^{(w)}$ at the BS is comprised of the remaining part of the model. Regarding the wireless channel setting, we use the additive white Gaussian noise (AWGN) and Rayleigh channels. Moreover, we adopt the assumption of a quasi-static fading model that the channel gain changes slowly and remains static during the transmission of each data sample. The channel coding and modulation in the physical layer comply with the 3GPP specification [23] to ensure compatibility with modern wireless communication systems. In particular, the low-density parity-check (LDPC) code is used for channel coding, and modulations of QPSK, 16QAM, 64QAM, and 256QAM are supported.

First, we train the model under both standard and wireless distributed learning. We adopt the differentiable quantization technique to enable training with LDPC codes and modulation. Specifically, in the back-propagation of the training process, the derivative of the quantization function is zero everywhere except at integers, where it is undefined. Therefore, to enable transmission techniques like coding and modulation, we must replace its derivative in the back-propagation. The study in [24] summarizes various differentiable quantization methods that empirically work well, such as the soft-max weighted quantization in [25] and replacing quantization by additive uniform noise in [26]. The empirical risk \hat{L} and $\hat{L}(s)$ are averaged on multiple training results. Furthermore, we calculate the average difference across multiple simulations to derive $\hat{g}(\mu, f) = \frac{1}{n} \sum_i |\hat{L}(s_i) - L|$. We approximate the upper bound \hat{G} via Algorithm 1 and compute the task outage probability p_e . The outcomes are summarized in Table I, with the parenthesis denoting the power of channel noise, modulation, and code

TABLE I
COMPARISON BETWEEN LOSS DIFFERENCE AND UPPER BOUND

Channel	$\hat{g}(\mu, f)$	\hat{G}	p_e	Acc	BER
AWGN (5dB,16QAM,R=1/2)	0.0350	0.0518	0.2881	0.8152	0.1263
AWGN (10dB,64QAM,R=1/2)	0.0124	0.0423	0.2697	0.8344	0.0670
AWGN (15dB,64QAM,R=3/4)	0.0034	0.0390	0.2620	0.8318	0.0406
Rayleigh (5dB,16QAM,R=3/8)	0.0443	0.0769	0.2856	0.8196	0.1458
Rayleigh (10dB,64QAM,R=5/12)	0.0270	0.0656	0.2746	0.8284	0.1076
Rayleigh (15dB,64QAM,R=2/3)	0.0222	0.0505	0.2721	0.8348	0.0944

rate. From the table, the actual wireless risk discrepancy is maintained within the theoretical upper bound across various channel conditions. Hence, it effectively validates the reliability of the theorem on the wireless risk discrepancy and the distributed learning system's inherent robustness. Additionally, the validation accuracy and the BER of wireless transmission are summarized in the last two columns. It can be seen that the wireless distributed learning still performs well under a large BER, demonstrating its robustness against wireless channel noise.

Additionally, we illustrate the task-aware ϵ -capacity resulting from the robustness in wireless distributed learning. Specifically, we perform the distributed learning task with a particular model in a wireless system at various transmission rates, achieved by employing different code rates and modulation schemes. To be compatible with the bit-level communication system, the output features of the encoder are converted into binary sequences during the inference process. In particular, the floating-point precision elements are quantized to 1-bit fixed-point binary representations. In Figure 2, we plot the performance curves with loss on the x-axis and rate on the y-axis for a clear presentation. The Shannon channel capacity C and the task-aware ϵ -capacity C_s in (18) are noted in the figures. According to Definition 1, we identify the complement of task outage set \mathcal{E}^c as the *task achievable region*. In the simulation, the loss is an average on the dataset, it is valid to assert that the task outage probability remains below p_e when $|\hat{l} - L| < G$. The task achievable region is shaded in the figures.

From the figures, there exists a transmission rate R with which the performance falls at the boundary of the task achievable region. Therefore, a successful task can be accomplished by employing such a transmission rate. Notably, the rate R surpasses the Shannon channel capacity C , thus corroborating the intrinsic robustness in wireless distributed learning. Furthermore, we compute the task-aware ϵ -capacity C_s in (18) using the task outage probability p_e from Table I. It can be seen from Figure 2 that the achievable rate R falls below C_s , aligning with the proposed theorem.

V. PROPOSED ROBUST TRAINING FRAMEWORK

As analyzed in Section II, a small wireless risk discrepancy indicates that the model is more robust against imperfect wireless channels. However, since the discrepancy is defined by expected statistical results, it is relatively difficult to estimate in advance. Therefore, the upper bound of the wireless risk discrepancy derived in Section III-A can serve as an alternative

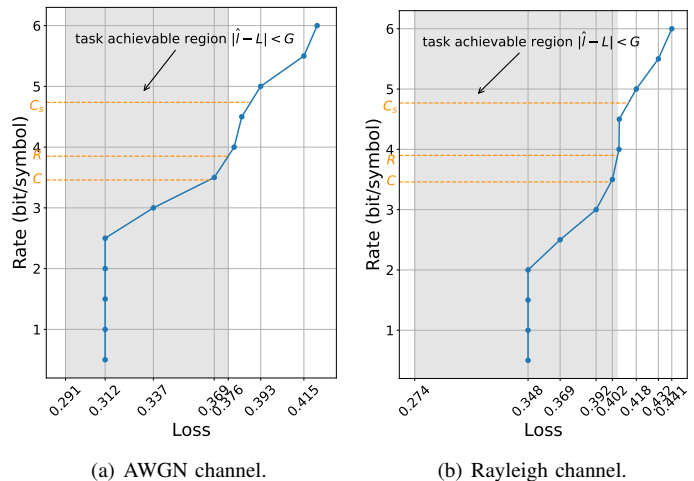


Fig. 2. The performance curves at different rates in AWGN and Rayleigh channels. The shadows denote the task achievable region.

to measuring the robustness of wireless distributed learning. By minimizing the upper bound $\sigma\sqrt{2I(W, Z; S)}$, the model could be generalized to various imperfect wireless channels while maintaining inference accuracy. For this purpose, we propose a robust training framework that optimizes the distributed feature decoder in an NN-based model scenario.

A. Accuracy and Robustness Trade-off

The mutual information $I(W, Z; S)$ is determined by the model weights, dataset, and the channel side information. For a specific task in wireless distributed learning, the dataset and the channel state are often given or fixed. Therefore, it is natural to minimize the mutual information in the training process by building an objective function as follows

$$\min_{p(w|s,z)} \mathbb{E}_{p(w|s,z)} \mathbb{E}_{p(s,z)} [l(W, Z)] + \beta I(W, Z; S). \quad (31)$$

The first term is the wireless risk considering the inference performance in the wireless distributed learning. The second one is mutual information in the derived upper bound, which aims to minimize the performance deterioration due to the wireless channel noise. The parameter $\beta > 0$ is the weight of the regularization term.

For classification tasks, the loss function becomes the cross entropy between the wireless prediction $p(y|x, w, s)$ and the target $p(y|x)$. As shown in [27], minimizing the cross-entropy

is equivalent to maximizing the mutual information. Hence, the objective function in (31) is equivalent to

$$\max_{p(w|s,z)} I(Y; W, S|X) - \beta I(W, Z; S). \quad (32)$$

Similar to the IB framework, the objective function demonstrates a trade-off between the sufficiency of information on the task target Y and the minimality of the learned weight W . This trade-off aims for learned weights that have minimal information about the channel state information to avoid overfitting while having sufficient information about the labels [28]. Specifically, the set of sufficient weights \mathcal{S} and minimal sufficient weights \mathcal{M} are defined as follows

$$\begin{aligned} \mathcal{S} &:= \arg \max_{W'} I(Y; W', S|X), \\ \mathcal{M} &:= \arg \min_{W' \in \mathcal{S}} I(W', Z; S). \end{aligned} \quad (33)$$

Based on the chain rule of conditional mutual information, the first term could be expanded as

$$I(Y; W, S|X) = I(Y; W|X) + I(Y; S|W, X). \quad (34)$$

Combined with (12), we have

$$I(Y; W, S|X) - I(Y; W|X) = I(W, Z; S) - I(W, X; S). \quad (35)$$

The second term on the right-hand side could be further expressed as $I(W, X; S) = I(X; S) + I(W; S|X) = I(W; S|X)$, where $I(X; S) = 0$ since Z and S are independent. It could be seen from (35) that the sufficiency $I(Y; W, S|X)$ increases with minimality $I(W, Z; S)$, thereby establishing the trade-off between them.

The objective function is a weighted sum of two mutual information terms with a parameter controlling the trade-off. Specifically, the inference accuracy is characterized by the amount of information about the task in the model weights. Intuitively, if the model learns more about the target and the wireless channel conditions, the BS could recover a high-quality feature leading to higher accuracy. However, as the minimal sufficient statistic in the IB framework, learning too much about the dataset may result in overfitting. Thus, there is an inherent trade-off between the inference performance and the robustness against channel distortions. The objective function in (32) formulates such an accuracy-robustness trade-off for the wireless distributed learning system.

B. Optimal Solution

Given the dataset Z and channel side information S , our goal is to find the optimal weights $p(w|s, z)$ that minimize the objective function. The variational method is a common way to solve the mutual information trade-off in (31). First, we consider the conditional distribution constraint of $p(w|s, z)$. The problem could be formulated as

$$\begin{aligned} \min_{p(w|s,z)} & \mathbb{E}_{p(w|s,z)} \mathbb{E}_{p(s,z)} [l(W, Z)] + \beta I(W, Z; S), \\ \text{s.t.} & \mathbb{E}[p(w|s, z)] = 1. \end{aligned} \quad (36)$$

Using the Lagrange multipliers method, we have the following lemma for the optimal solution.

Lemma 3. *The optimal posterior $p(w|s, z)$ that minimizes (31) satisfies the equation*

$$p(w|s, z) = \frac{p(w|z)}{A(s, z)} \exp\left(-\frac{1}{\beta} \hat{L}_{s,z}(w)\right), \quad (37)$$

where $A(s, z)$ is a normalizing constant.

Proof. By introducing the Lagrange multipliers $\lambda(s, z)$ for the normalization of the conditional distribution, the Lagrangian function could be written as

$$\begin{aligned} \mathcal{L} &= \mathbb{E}_{p(w|s,z)} [\hat{L}_{s,z}(w)] + \beta \mathbb{E}_{p(w,s,z)} \left[\frac{\log p(w|s, z)}{p(w|z)} \right] \\ &+ \mathbb{E}_{p(s,z)} \lambda(s, z) (\mathbb{E}[p(w|s, z)] - 1), \end{aligned} \quad (38)$$

where the empirical wireless risk given a certain dataset and channel condition is denoted as $\hat{L}_{s,z}(w) = \frac{1}{n} \sum_{i=1}^n l(\hat{y}_i, y_i)$. Additionally, the fact in (12) that $I(W, Z; S) = I(W; S|Z)$ is adopted. Taking derivatives with respect to the posterior $p(w|s, z)$ for given s and z results in

$$\frac{\partial \mathcal{L}}{\partial p(w|s, z)} = \hat{L}_{s,z}(w) + \beta \left(\frac{\log p(w|s, z)}{p(w|z)} - 1 \right) + \lambda(s, z). \quad (39)$$

Let $\frac{\partial \mathcal{L}}{\partial p(w|s, z)} = 0$ and the variational result could be obtained, as follows

$$\begin{aligned} \log p(w|s, z) &= -\frac{1}{\beta} \hat{L}_{s,z}(w) + \log p(w|z) - \tilde{\lambda}(s, z), \\ p(w|s, z) &= p(w|z) \exp\left(-\frac{1}{\beta} \hat{L}_{s,z}(w)\right) \exp\left(-\tilde{\lambda}(s, z)\right), \end{aligned} \quad (40)$$

where $\tilde{\lambda}(s, z) = \frac{\lambda(s, z)}{\beta} + 1$. The second exponential term $\exp(-\tilde{\lambda}(s, z))$ could be considered as the partition function that normalizes the conditional distribution. Let the normalized function $A(s, z)$ be defined as

$$\begin{aligned} A(s, z) &= \exp\left(-\tilde{\lambda}(s, z)\right) \\ &= \mathbb{E} \left[p(w|z) \exp\left(-\frac{1}{\beta} \hat{L}_{s,z}(w)\right) \right], \end{aligned} \quad (41)$$

thereby completing the proof. \square

To obtain the optimal posterior in (37), we express it in the exponential form

$$p(w|s, z) = \frac{1}{A(s, z)} \exp\left(\frac{1}{\beta} U(w)\right), \quad (42)$$

where $U(w) = \hat{L}_{s,z}(w) - \beta \log p(w|z)$. This reveals that $p(w|s, z)$ follows a typical Gibbs distribution $\pi(w) \propto \exp(-kU(w))$ with an energy function $U(w)$ and a temperature parameter β corresponded to the regularization term in (31). According to [29], if U has a unique global minimum, is sufficiently smooth, and properly behaved at the boundaries, the Langevin diffusion $X(t)$ in the following stochastic differential equation converges to the stationary distribution $\pi(x) \propto \exp\left(-\frac{1}{\beta} U(x)\right)$

$$dX(t) = -\nabla U(X(t))dt + \sqrt{2\beta} dB(t), \quad t \geq 0, \quad (43)$$

where $B(t)$ is the standard Brownian motion in \mathbb{R}^D . Specifically, the Gibbs distribution is the unique invariant distribution of (43), and the distribution of $X(t)$ converges rapidly to $\pi(x)$ as $t \rightarrow \infty$. Furthermore, for sufficiently small values of temperature β , the Gibbs distribution concentrates around the minimum of U . Thus, with high probability, a sample from the Gibbs distribution is an almost-minimizer of the energy function $U(X(t))$ [30].

Applying the Euler-Maruyama discretization [31] to (43) yields the discrete-time Markov process:

$$X_{k+1} = X_k - \eta_k g_k + \epsilon_k \cdot \sqrt{2\eta_k \beta}, \quad (44)$$

where g_k is a conditionally unbiased estimate of the energy function gradient $\nabla U(X_k)$, $\epsilon_k \sim \mathcal{N}(\mathbf{0}, \mathbf{I}_D)$ is a standard Gaussian noise vector, and $\eta_k > 0$ is the step size. This recursion corresponds to the weight update process of Stochastic Gradient Langevin Dynamics (SGLD) [32]. It has been demonstrated in [33], [34] that the discrete SGLD recursion accurately tracks the Langevin diffusion. Under the conditions $\sum_t \eta_t \rightarrow \infty$, $\sum_t \eta_t^2 \rightarrow 0$, and an annealing temperature β , the distribution of X_k will approximate the Gibbs distribution for sufficiently large k . Therefore, for large enough k , the output of the SGLD algorithm is also an almost-minimizer of the energy function $U(X_k)$.

Consequently, it is natural to adopt the SGLD algorithm to approximate the optimal posterior $p(w|s, z)$ by setting the model weights w as the Langevin diffusion X_k . The SGLD algorithm is capable of efficiently and effectively solving large-scale posterior inference, achieving an exponential rate of convergence for a non-convex objective function [33]. Therefore, we can utilize the update process in (44) to iteratively calculate the optimal weights by $w_{k+1} = w_k - \eta_k \nabla U(w) + \sqrt{2\eta_k \beta} \epsilon_k$. To calculate the energy function $U(w) = \hat{L}_{s,z}(w) - \beta \log p(w|z)$, we adopt the assumption in Section IV that $p(w|z) = \mathcal{N}(w|\theta_z, \Sigma_z)$ is a Gaussian distribution in the deep learning scenario. Thus, we have

$$-\log p(w|z) \propto (w - \theta_z)^\top \Sigma_z^{-1} (w - \theta_z) + \log \det \Sigma_z, \quad (45)$$

where the determinant term is equivalent to the sum of the logarithm of eigenvalues $\log \det \Sigma_z = \sum_{i=1}^D \lambda_i$. The detailed SGLD training process for the proposed objective function (31) is summarized in Algorithm 2.

Algorithm 2 SGLD training process

Require: Number of samples n , number of batches B , learning rate η , temperature β , decay scheme ϕ_η, ϕ_β .

Ensure: Model weights $\{w_k\}$ satisfying $p(w|s, z)$.

- 1: Pre-train in standard distributed learning, $\theta_z \leftarrow p(w|z)$.
 - 2: **repeat**
 - 3: Calculate the mini-batch gradient of energy function $g_{k-1} \leftarrow \nabla \left(-\frac{B}{n} \sum_b \log p(y_b|x_b, w_{k-1}, s_b) - \beta_{k-1} \log p(w_{k-1}|z) \right)$.
 - 4: Sample Gaussian random noise $\epsilon_k \leftarrow \mathcal{N}(\mathbf{0}, \mathbf{I}_D)$.
 - 5: Weights update $w_k \leftarrow w_{k-1} - \eta_{k-1} g_k + \epsilon_k \cdot \sqrt{2\eta_{k-1} \beta_{k-1}}$.
 - 6: Learning rate and temperature decay $\eta_k \leftarrow \phi_\eta(\eta_{k-1}), \beta_k \leftarrow \phi_\beta(\beta_{k-1})$.
 - 7: $k \leftarrow k + 1$.
 - 8: **until** The weights $\{w_k\}$ converge.
-

VI. SIMULATIONS

In this section, we evaluate the performance of the proposed robust training framework in Section V by comparing it with the vanilla training mechanism.

A. Robustness Evaluation

To evaluate the performance of the proposed robust training framework, we conduct the image classification task on multiple datasets using different NN models.

1) **Datasets:** In this section, we select three benchmark datasets for image classification, including ASIRRA Cats & Dogs, CIFAR-10 and CIFAR-100 [35]. The CIFAR-10 dataset consists of 60,000 color images in 10 classes with 6,000 images per class, including 50,000 training images and 10,000 test images. The CIFAR-100 dataset consists of the same number of color images as CIFAR-10, but it has 100 classes with 600 images per class. There are 500 training images and 100 testing images per class. The 100 classes in the CIFAR-100 are grouped into 20 superclasses. Each image comes with a "fine" label (the exact class) and a "coarse" label (the superclass). For the classification tasks, we adopt classification accuracy as the performance metric.

2) **NN architectures:** To demonstrate the effectiveness of the proposed robust training framework, we implement the wireless distributed learning system with two classic CNNs, the VGG network [36] and the Residual Network (ResNet) [37]. Specifically, we utilize VGG11 and ResNet18 models for the CIFAR-10 classification task, while VGG16 and ResNet34 models are employed for the CIFAR-100 classification task. As for the Cats & Dogs dataset, the 6-layer CNN in Section IV is adopted. The detailed architectures for the encoder $f_e^{(W)}$ and decoder $f_d^{(W)}$ are presented in Appendix B.

3) **Baseline:** We compare the proposed robust training framework in wireless distributed learning against the vanilla training technique. In particular, the vanilla method trains NNs with plain cross entropy loss and Adam optimizer [38], which is a well-recognized stochastic optimization method.

4) **Communication system:** In this experiment, we assume a flat-fading channel for the wireless environment. Similar to the wireless settings in Section IV, the physical layer complies with the 3GPP standard. For simplicity, we only adopt modulation during the transmission process, including BPSK, QPSK, 8QAM, 16QAM, 32QAM, and 64QAM. To align with the modern communication system, the differentiable quantization technique is also adopted to enable training with modulation. As for the wireless inference, we normalize the output features of the encoder and quantize the floating-point precision features into 1-bit fixed-point binary representations.

We first jointly train the encoder and the decoder on the corresponding dataset. Next, we fine-tune the model using both Algorithm 2 and vanilla Adam in wireless distributed learning where the SNR of the channel is 10dB and the

modulation scheme is QPSK. During the training process, we record the accuracy on the test dataset and calculate the mutual information $I(W; Z; S)$ in the derived upper bound using Algorithm 1. To demonstrate the superiority of our proposed robust training framework in terms of robustness against channel distortions, we compare the inference accuracy of the trained models in wireless distributed learning. Specifically, we conduct the wireless distributed learning in a channel at an SNR of 10dB using multiple transmission rates, achieved by employing different modulation schemes. The task-aware ϵ -capacity derived in (18) results from the inherent robustness in wireless distributed learning. Given the enhanced robustness using the proposed robust training framework, we could achieve higher task-aware ϵ -capacity and thus boost communication efficiency.

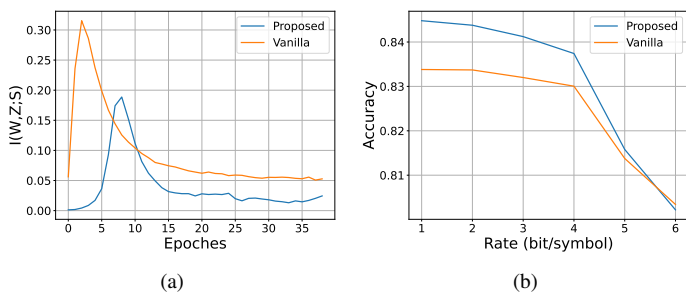


Fig. 3. 6-layer CNN on Cats & Dogs Dataset. (a): The approximated mutual information $\hat{I}(W, Z; S)$ of the upper bound during the training. (b): The accuracy on the test dataset w.r.t the transmission rates.

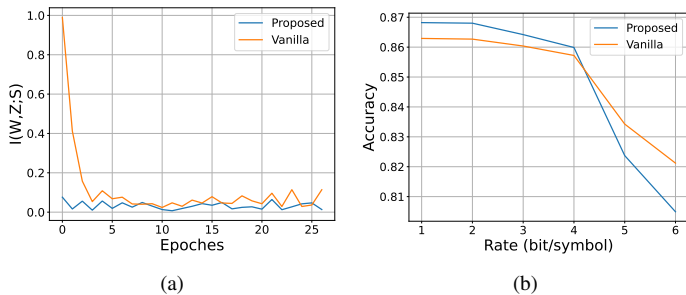


Fig. 4. VGG11 on CIFAR-10 Dataset. (a): The approximated mutual information $\hat{I}(W, Z; S)$ of the upper bound during the training. (b): The accuracy on the test dataset w.r.t the transmission rates.

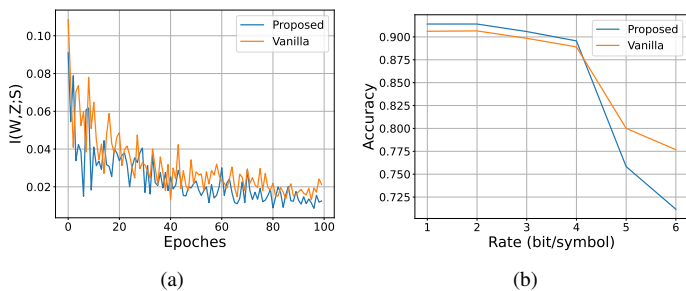


Fig. 5. ResNet18 on CIFAR-10 Dataset. (a): The approximated mutual information $\hat{I}(W, Z; S)$ of the upper bound during the training. (b): The accuracy on the test dataset w.r.t the transmission rates.

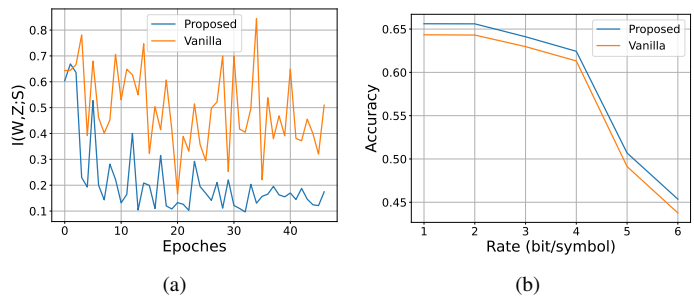


Fig. 6. VGG16 on CIFAR-100 Dataset. (a): The approximated mutual information $\hat{I}(W, Z; S)$ of the upper bound during the training. (b): The accuracy on the test dataset w.r.t the transmission rates.

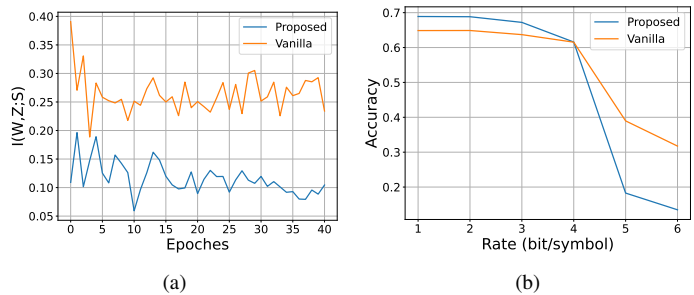


Fig. 7. ResNet34 on CIFAR-100 Dataset. (a): The approximated mutual information $\hat{I}(W, Z; S)$ of the upper bound during the training. (b): The accuracy on the test dataset w.r.t the transmission rates.

The training and inference results are summarized in Figures 3-7. From the figures, the mutual information $I(W, Z; S)$ decreases over the epochs and converges to a small value. This is because the NN's weights are continuously updated throughout the training process, causing the mutual information to change. It eventually stabilizes as the optimal weights of NN are learned. This suggests that the training process enhances the inherent robustness of NN against wireless distortion. It can be seen from the figures that the proposed robust training framework achieves a smaller upper bound $G = \sigma\sqrt{2I(W, Z; S)}$ in training and thus improves the robustness of the wireless distributed learning. Additionally, we could see from the result of the simple CNN in Figure 3(a) that the mutual information $I(W, Z; S)$ surges in the first few training epochs, and then decreases slowly approaching zero. Such a phenomenon corresponds to the 'fitting' and 'compression' hypothesis in the IB theory of deep learning [39], where the model learns information about the task in the fitting phase and increases the generalization performance in the compression phase. The training process of the robust training framework could also be divided into two phases according to the curve of mutual information $I(W, Z; S)$. In the first phase, as analyzed in (12), $I(W, Z; S)$ increases since the model extracts all information from the wireless channel and the wireless inference task. In the second phase, the model starts to abandon the irrelevant information and regularize the wireless discrepancy gap between the wireless risk and standard risk. However, for deeper and more complex NNs, the first fitting phase could be too short and could not be observed in the experiments.

Comparing the test accuracy in the inference process, the model trained in the robust training framework outperforms the baseline. We credit the improvement to the explicit consideration of information regularization during the training process, which enhances the model’s generalization ability to various channel conditions. In our experiment, the channel capacity at an SNR of 10dB is approximately 3.46 bit/symbol. The conventional communication system requires a rate of 3 bit/symbol for error-free transmission. The simulation results indicate that the proposed framework achieves higher task accuracy up to the rate of 4 bit/symbol, enabling the learning model to transmit at a rate beyond the Shannon capacity while maintaining inference accuracy. It demonstrates that we could leverage the intrinsic robustness within wireless distributed learning for higher communication efficiency while maintaining the inference performance. Therefore, the proposed robust training framework could effectively enhance the robustness of wireless distributed learning, thereby exploiting this robustness to transcend the Shannon capacity. However, it is worth noting that the task accuracy for both the proposed and vanilla methods declines rapidly at high transmission rates above 4 bit/symbol. In some cases, the proposed framework may even underperform compared to the vanilla method. This is because the transmission rate exceeds the proposed task-aware ϵ -capacity, leading to a high task outage probability. Such a scenario is outside the scope of this study, which primarily focuses on theoretically exploring the task-aware transmission upper limit that slightly exceeds the Shannon capacity by leveraging the robustness in wireless distributed learning.

VII. CONCLUSION

In this paper, we have presented an information-theoretic analysis of the robustness within wireless distributed learning and its implications for achieving task-aware ϵ -capacity. By leveraging information theory, we derived an upper bound in terms of mutual information on the performance deterioration due to the wireless fading. The upper bound serves as a measure of the robustness against channel distortions. In contrast to the bit-level metric, we defined task outage based on the upper bound as a metric for successful inference. Thereby, we characterized the maximum achievable rate in wireless distributed learning and the task-aware ϵ -capacity benefiting from robustness. We further proposed an efficient algorithm to estimate the upper bound in practice. Given the theoretical analysis of the robustness in wireless distributed learning, we design a robust training framework based on the derived upper bound, which is capable of improving the model’s robustness. The robustness in wireless distributed learning and the effectiveness of our framework are validated through numerical experiments.

APPENDIX A PROOF OF COROLLARY 1

Proof. Leveraging the Donsker-Varadhan variational representation in (5), we have

$$\begin{aligned} D_{\text{KL}}(q(w, z|s)||p(w, z)) \\ \geq \lambda (\mathbb{E}_q[l(W, Z)] - \mathbb{E}_p[l(W, Z)]) - \frac{\lambda^2 \sigma^2}{2(1 - c\lambda)}. \end{aligned} \quad (46)$$

For simple notation, we denote $D_{\text{KL}}(q(w, z|s)||p(w, z))$ as $D(q||p)$. Following the same proof in Theorem 1 that the discriminant must be non-positive, we have

$$[cD(q||p) - (\mathbb{E}_q[l(W, Z)] - \mathbb{E}_p[l(W, Z)])]^2 \leq 2\sigma^2 D(q||p). \quad (47)$$

Therefore, the difference between expectations can be upper-bounded as follows

$$\mathbb{E}_q[l(W, Z)] - \mathbb{E}_p[l(W, Z)] \leq \sigma \sqrt{2D(q||p)} + cD(q||p). \quad (48)$$

Taking the expectation under the side information distribution μ and utilizing Jensen’s inequality gives

$$\begin{aligned} \mathbb{E}_\mu[\mathbb{E}_q[l(W, Z)] - \mathbb{E}_p[l(W, Z)]] \\ \leq \mathbb{E}_\mu[\sigma \sqrt{2D(q||p)} + cD(q||p)] \\ \leq \sqrt{2\sigma^2 \mathbb{E}_\mu[D(q||p)]} + cI(W, Z; S) \\ = \sigma \sqrt{2I(W, Z; S)} + cI(W, Z; S). \end{aligned} \quad (49)$$

This completes the proof. \square

APPENDIX B EXPERIMENT SETTINGS

In wireless distributed learning, the NN model $f^{(W)}$ is separated into an encoder $f_e^{(W)}$ at the UE and a decoder $f_d^{(W)}$ at the BS. The detailed deployment of the models in the experiment, including VGG11, VGG16, ResNet18, and ResNet34, is summarized in Table II.

REFERENCES

- [1] J. Shao, Y. Mao, and J. Zhang, “Learning task-oriented communication for edge inference: An information bottleneck approach,” *IEEE J. Sel. Areas Commun.*, vol. 40, no. 1, pp. 197–211, Jan. 2022.
- [2] N. Farsad, M. Rao, and A. Goldsmith, “Deep learning for joint source-channel coding of text,” in *Proc. IEEE Int. Conf. Acoust. Speech Signal Process. (ICASSP)*, pp. 2326–2330, Apr. 2018.
- [3] E. Boursoulatzé, D. B. Kurka, and D. Gündüz, “Deep joint source-channel coding for wireless image transmission,” *IEEE Trans. Cogn. Commun. Netw.*, vol. 5, no. 3, pp. 567–579, Sep. 2019.
- [4] H. Xie, Z. Qin, G. Y. Li, and B.-H. Juang, “Deep learning enabled semantic communication systems,” *IEEE Trans. Signal Process.*, vol. 69, pp. 2663–2675, 2021.
- [5] J. Bao, P. Basu, M. Dean, C. Partridge, A. Swami, W. Leland, and J. A. Hendlér, “Towards a theory of semantic communication,” in *Proc. IEEE Netw. Sci. Workshop*, Jun. 2011, pp. 110–117.
- [6] L. Xia, Y. Sun, D. Niyato, X. Li, and M. A. Imran, “Joint user association and bandwidth allocation in semantic communication networks,” *IEEE Trans. Veh. Technol.*, vol. 73, no. 2, pp. 2699–2711, Feb. 2024.
- [7] J. Liu, W. Zhang, and H. V. Poor, “A rate-distortion framework for characterizing semantic information,” in *Proc. IEEE Int. Symp. Inf. Theory (ISIT)*, Jul. 2021, pp. 2894–2899.
- [8] Y. Shao, Q. Cao, and D. Gündüz, “A theory of semantic communication,” *IEEE Transactions on Mobile Computing*, to be published.

TABLE II
NN ARCHITECTURE IN WIRELESS DISTRIBUTED LEARNING

Model	encoder	decoder
6-layer CNN	Conv16+Conv32+Conv64	FC500*2+FC50+FC2
VGG11	Conv64+Conv128+Conv256×2+Conv512×2	Conv512×2+FC4096+FC4096+FC10
VGG16	Conv64×2+Conv128×2+Conv256×3	Conv512×3+Conv512×3+FC4096*2+FC4096+FC100
ResNet18	Conv64+Block64×2*3+Block128×2	Block256×2+Block512×2+FC10
ResNet34	Conv64+Block64×3+Block128×4	Block256×6+Block512×3+FC10

*1 Conv represents a convolutional layer with kernel size 3×3 , and 16 represents the number of channels.

*2 FC represents a full connected layer.

*3 Block represents a residual block with two convolutional layers and a skip connection, and 64 represents the number of channels of the convolutional layers.

- [9] Y. He, G. Yu, and Y. Cai, "Rate-adaptive coding mechanism for semantic communications with multi-modal data," *IEEE Trans. Commun.*, vol. 72, no. 3, pp. 1385–1400, Mar. 2024.
- [10] R. M. Gray, *Entropy and information theory*. Berlin, Germany: Springer Science & Business Media, 2011.
- [11] P. Rigollet and J.-C. Hütter, "High-dimensional statistics," *arXiv preprint arXiv:2310.19244*, 2023.
- [12] A. Xu and M. Raginsky, "Information-theoretic analysis of generalization capability of learning algorithms," in *Proc. Adv. Neural Inf Process. Syst. (NIPS)*, Dec. 2017, pp. 2521–2530.
- [13] Z. Wang, S.-L. Huang, E. E. Kuruoglu, J. Sun, X. Chen, and Y. Zheng, "PAC-bayes information bottleneck," in *Proc. Int. Conf. Learn. Represent. (ICLR)*, Apr. 2022.
- [14] Z. Goldfeld, E. Van Den Berg, K. Greenewald, I. Melnyk, N. Nguyen, B. Kingsbury, and Y. Polyanskiy, "Estimating information flow in deep neural networks," in *Proc. Int. Conf. Mach. Learn. (ICML)*, Jun. 2019, pp. 2299–2308.
- [15] G. Zhang, Q. Hu, Y. Cai, and G. Yu, "Scan: Semantic communication with adaptive channel feedback," *IEEE Trans. Cogn. Commun. Netw.*, vol. 10, no. 5, pp. 1759–1773, Oct. 2024.
- [16] T. M. Getu, W. Saad, G. Kaddoum, and M. Bennis, "Performance limits of a deep learning-enabled text semantic communication under interference," *IEEE Trans. Wirel. Commun.*, vol. 23, no. 8, pp. 10213–10228, Aug. 2024.
- [17] D. Tse and P. Viswanath, *Fundamentals of Wireless Communication*. Cambridge, U.K.: Cambridge Univ. Press, 2005.
- [18] S. Verdú and T. S. Han, "A general formula for channel capacity," *IEEE Trans. Inf. Theory*, vol. 40, no. 4, pp. 1147–1157, Jul. 1994.
- [19] G. K. Dziugaite and D. M. Roy, "Data-dependent pac-bayes priors via differential privacy," in *Proc. Adv. Neural Inf Process. Syst. (NIPS)*, Dec. 2018, pp. 8440–8450.
- [20] P. W. Koh and P. Liang, "Understanding black-box predictions via influence functions," in *Proc. Int. Conf. Mach. Learn. (ICML)*, Aug. 2017, pp. 1885–1894.
- [21] R. D. Cook and S. Weisberg, *Residuals and Influence in Regression*. New York, USA: Chapman and Hall, 1982.
- [22] W. Cukierski, "Dogs vs. cats," 2013. [Online]. Available: <https://kaggle.com/competitions/dogs-vs-cats>
- [23] 3GPP, "NR; Physical layer procedures for data," Technical Specification (TS) 36.214, Version 17.2.0.
- [24] L. Theis, W. Shi, A. Cunningham, and F. Huszár, "Lossy image compression with compressive autoencoders," in *Proc. Int. Conf. Learn. Represent. (ICLR)*, Apr. 2017.
- [25] E. Agustsson, F. Mentzer, M. Tschannen, L. Cavigelli, R. Timofte, L. Benini, and L. Van Gool, "Soft-to-hard vector quantization for end-to-end learning compressible representations," in *Proc. Adv. Neural Inf Process. Syst. (NIPS)*, Dec. 2017, pp. 1141–1151.
- [26] J. Ballé, V. Laparra, and E. P. Simoncelli, "End-to-end optimization of nonlinear transform codes for perceptual quality," in *Proc. Picture Coding Symp. (PCS)*, Dec. 2016, pp. 1–5.
- [27] M. Boudiaf, J. Rony, I. M. Ziko, E. Granger, M. Pedersoli, P. Piantanida, and I. B. Ayed, "A unifying mutual information view of metric learning: Cross-entropy vs. pairwise losses," in *Proc. Eur. Conf. Comput. Vis.*, Aug. 2020, pp. 548–564.
- [28] O. Shamir, S. Sabato, and N. Tishby, "Learning and generalization with the information bottleneck," *Theor. Comput. Sci.*, vol. 411, no. 29–30, pp. 2696–2711, Jun. 2010.
- [29] T.-S. Chiang, C.-R. Hwang, and S. J. Sheu, "Diffusion for global optimization in R^n ," *SIAM J. Control Optim.*, vol. 25, no. 3, pp. 737–753, May 1987.
- [30] C.-R. Hwang, "Laplace's method revisited: Weak convergence of probability measures," *Ann. Probab.*, vol. 8, no. 6, pp. 1177–1182, Dec. 1980.
- [31] P. E. Kloeden and E. Platen, *Numerical Solution of Stochastic Differential Equations*, Berlin, Germany: Springer, 1992.
- [32] M. Welling and Y. W. Teh, "Bayesian learning via stochastic gradient langevin dynamics," in *Proc. Int. Conf. Mach. Learn. (ICML)*, Jun. 2011, pp. 681–688.
- [33] M. Raginsky, A. Rakhlin, and M. Telgarsky, "Non-convex learning via stochastic gradient langevin dynamics: A nonasymptotic analysis," in *Proc. Conf. Learn. Theory*, Jul 2017, pp. 1674–1703.
- [34] P. Xu, J. Chen, D. Zou, and Q. Gu, "Global convergence of langevin dynamics based algorithms for nonconvex optimization," in *Proc. Adv. Neural Inf Process. Syst. (NIPS)*, Dec. 2018, pp. 3126–3137.
- [35] A. Krizhevsky, G. Hinton et al., "Learning multiple layers of features from tiny images," Univ. Toronto, Toronto, Ontario, 2009.
- [36] K. Simonyan and A. Zisserman, "Very deep convolutional networks for large-scale image recognition," *arXiv preprint arXiv:1409.1556*, 2014.
- [37] K. He, X. Zhang, S. Ren, and J. Sun, "Deep residual learning for image recognition," in *Proc. IEEE Conf. Comput. Vis. Pattern Recognit. (CVPR)*, Jun. 2016, pp. 770–778.
- [38] D. P. Kingma and J. Ba, "Adam: A method for stochastic optimization," *Proc. Int. Conf. Learn. Represent. (ICLR)*, 2014.
- [39] A. A. Alemi, I. Fischer, J. V. Dillon, and K. Murphy, "Deep variational information bottleneck," in *Proc. Int. Conf. Learn. Represent. (ICLR)*, Apr. 2017.